PHYSICAL REVIEW A VOLUME 17, NUMBER 6 JUNE 1978

Application of the close-coupling method to excitation of electronic states and dissociation of H_2 by electron impact

Sunggi Chung and Chun C. Lin
Department of Physics, University of Wisconsin, Madison, Wisconsin 53706
(Received 10 January 1978)

The close-coupling method has been applied to the electron-H_2 collision to obtain excitation cross sections of the $b\,^3\Sigma_u^+$, $a\,^3\Sigma_g^+$, $e\,^3\Sigma_u^+$, $c\,^3\Pi_u$, and $B\,^1\Sigma_u^+$ states. Cross sections of the triplet states are presented at several incident-electron energies between threshold and 40 eV, and those of the $B\,^1\Sigma_u^+$ state at 25, 50, 75, and 100 eV. Vibrational levels are treated by the Franck-Condon-factor approximation, and the cross sections are rotationally averaged. Cross sections by the Born-type calculations are markedly different from those of the present calculation. Furthermore, the manner and degree to which they differ also vary from state to state. Comparison with experiment is limited to a set of experimental data of total dissociation cross sections.

I. INTRODUCTION

Excitation of the electronic states of a molecule by electron impact is one of the simplest basic processes in molecular-collision phenomena. The importance of such excitation processes in many areas of studies has stimulated considerable experimental efforts in recent years. However, the progress in the theoretical aspects of the problem has been much slower. In fact, the status of the theory of electron-impact excitation of the electronic states of diatomic molecules is in a rather primitive stage in comparison with the corresponding electron-atom processes. For a few diatomic molecules (H_2, N_2, CO), systematic studies[1-8] of the excitation cross sections for a number of singlet and triplet states have been made by means of the Born approximation and/or the modified versions of it. The modifications of the Born approximation as introduced by Ochkur[9] and by Rudge[10] enable one to handle the exchange interaction between the colliding and the target electrons in a simple way. Excitation from a singlet to another singlet state can be treated either by the first Born approximation (referred to as the Born approximation in this paper), or by one of the modified versions when the exchange effect is included. On the other hand, one must resort to the Born-Ochkur or the Born-Rudge approximation for excitation to triplet states. In Refs. 1 and 2, it is suggested that Born-Ochkur approximation be used for singlet-singlet excitation, but the Born-Rudge scheme is recommended for singlet-triplet processes. Comparison with experiments shows satisfactory agreement for a few states, but rather large discrepancy is found for some others. Viewed as a whole, one can only regard the Born-type calculation as a means of providing theoretical estimates but not always cross sections of precise quantitative significance. In the cases of singlet-triplet processes, the excitation functions generally peak at a few eV above the threshold and decrease steeply with increasing energy. For many applications, the major interest in triplet excitation lies in the near-threshold region where the cross sections are large, but this is also the region in which the validity of the Born approximation becomes questionable. Recently a calculation based on "the first-order many-body formula" (a form of distorted-wave approximation) was advanced,[11] which is yet to be tested against more rigorous theories. Like the Born-Ochkur and Born-Rudge approximations before it, this method, too, takes advantage of relative simplicity in computation but also falls short of serious theoretical justification. Collectively, these efforts are a testimony that while the need for theoretical cross sections is great, the means of obtaining them is restricted—no doubt, due to the computational complexity involved in the molecular problems.

The most rigorous and systematic formalism commonly applied to the electron-atom collision processes is the method of close coupling.[12-17] About ten years ago a very ambitious effort of applying the close-coupling method to electron-H_2 excitation was undertaken by Fajen.[18] He calculated the excitation cross sections of the $B\,^1\Sigma_u^+$, $C\,^1\Pi_u$, and $E\,^1\Sigma_g^+$ states of H_2 by a multistate close coupling scheme. To make the problem tractable, Fajen neglected the exchange interaction between the colliding and target electrons. The emphasis of his work is mainly focused on the problem of singlet-singlet excitation in the high and intermediate energies, particularly the effect of multistate indirect coupling on the cross sections of the $E\,^1\Sigma_g^+$ state. Black and Lane[19,20] also calculated the cross sections of the $B\,^1\Sigma_u^+$ state by the close-coupling method. The electron exchange was ap-

proximated as an effective exchange potential by the scaled Slater-Hartree-Fock form to simplify the computation.[20] The latter work was primarily concerned with the resonant excitation of the $B\,^1\Sigma_u^+$ state at low incident-electron energies (11–13 eV).

In this paper we apply the method of close coupling to the electron-H_2 problem with the projectile-target electron exchange included, and calculate excitation cross sections for several triplet states as well as the $B\,^1\Sigma_u^+$ state. The theoretical formulation and the computational procedures parallel closely those of the atomic cases with two notable differences coming from the axial symmetry of molecule and the two-center nature of (homonuclear diatomic) molecular wave functions. From the computational standpoint, these differences translate into one additional truncation of an infinite sum beyond the atomic calculation. In our calculations this truncation is fully justified with a demonstrated convergence. Aside from this point, all computations are carried out to the same degree of refinement as the corresponding electron-atom problems.

II. GENERAL THEORY

The development of the close-coupling theory dates back to the 1950's.[12] Since then this method has been applied with increasing frequency to electron-atom problems,[13-17] so that the general theory of the close-coupling method is rather well known now. Nevertheless, for the purpose of later discussions, we specialize it to electron–diatomic-molecule collision processes which result in an excitation of electronic states. The formulation here parallels closely to those already published in conjunction with the electron-atom case, particularly, the work by Smith, Henry, and Burke.[14]

In the field of electron-molecule collision, when an excitation is made from one electronic state to another, we are interested in the excitation cross sections that are averaged over the initial rotational substates, and summed over the final rotational substates. In order to compute such cross sections, it is possible—in fact desirable from the computational point of view—to formulate the problem in the molecule-fixed frame of reference,[21,22] thereby ignoring the rotational structure completely. However, in its stead, we average the direction of the incident electron with respect to the orientation of molecule. The only assumption needed here is that the energy of scattered electrons be much greater than the energy spacings of the rotational states.

As to the treatment of the vibrational motion, it is a common practice to use the Franck-Condon-factor approximation, by which electronic states of molecules are considered "vibrationless." This simplifies the calculation, since the vibrational wave functions now enter the computation only through Franck-Condon (FC) factors so that the scattering equations can be solved without the knowledge of vibrational motion. A discussion concerning the validity of this approximation will be given at the end of this paper. In the present work we will focus our attention to the electronic motion and ignore the dependency of electronic functions on the internuclear distance. Thus, in what follows, all electronic functions are those corresponding to the equilibrium separation of the ground state.

An electronic state of a diatomic molecule is defined by the angular momentum along the molecular axis λ, and the spin (sm). We use n to distinguish different states which have the same quantum numbers (λsm). Thus, we write an N-electron electronic wave function as

$$\Phi(n\lambda sm\,|\vec{\mathbf{x}}_1,\ldots,\vec{\mathbf{x}}_N)\,, \tag{1}$$

where $\vec{\mathbf{x}}_i$ represents the spatial $(\vec{\mathbf{r}}_i)$ and spin (σ_i) coordinates of the ith electron. Φ's are fully antisymmetrized products consisting of one-electron molecular orbitals $\phi_j(n_j\lambda_j|\vec{\mathbf{r}})$ with α or β spin, and they are assumed to satisfy the Schrödinger equation exactly

$$H_{\rm mol}\Phi(n\lambda sm)=E_{n\lambda}\Phi(n\lambda sm)\,, \tag{2}$$

$$H_{\rm mol}=-\sum_{i=1}^{N}\left[\tfrac{1}{2}\nabla_i^2+Z(|\vec{\mathbf{r}}_A-\vec{\mathbf{r}}_i|^{-1}+|\vec{\mathbf{r}}_B-\vec{\mathbf{r}}_i|^{-1})\right]+\sum_{i=1}^{N-1}\sum_{j=i+1}^{N}|\vec{\mathbf{r}}_i-\vec{\mathbf{r}}_j|^{-1}\,, \tag{3}$$

where Z is the nuclear charge, and $\vec{\mathbf{r}}_A$ and $\vec{\mathbf{r}}_B$ are the position vectors of the two nuclei. The scattered-electron wave is characterized by angular momenta (lm') and spin $(s=\frac{1}{2}, m=\pm\frac{1}{2})$.

The essence of the close-coupling method consists of expanding the total $(N+1)$-electron function of the collision system in terms of a suitable set of basis functions. Due to the axially symmetric field in which these $N+1$ electrons move, the total angular momentum projected on the molecular axis $\Lambda=\lambda+m'$ is a constant of the collision process. As we deal only with spin-independent Hamiltonians, the total spin (SM) are good quantum numbers. In fact the cross sections are independent of M.

Accordingly, we adopt a basis set which are eigenfunctions of $(SM\Lambda)$, i.e.,

$$\psi_{\mu}^{SM\Lambda}(X^{-i}) \equiv \psi_{n\lambda l s}^{SM\Lambda}(\vec{x}_1, \ldots, \hat{r}_i\sigma_i, \ldots, \vec{x}_{N+1})$$
$$= \sum_m C(s, \tfrac{1}{2}, m, M-m \,|\, SM) \times Y_{l,\Lambda-\lambda}(\hat{r}_i)\xi(\tfrac{1}{2}, M-m \,|\, \sigma_i) \times \Phi(n\lambda s m \,|\, \vec{x}_1, \ldots, \vec{x}_{i-1}, \vec{x}_{i+1}, \ldots, \vec{x}_{N+1}), \quad (4)$$

where $C(j_1 j_2 m_1 m_2 | JM)$ is the Clebsch-Gordan coefficient, Y_{lm} is the spherical harmonic and ξ is α- or β-spin function. We also used two shorthand notations: X^{-i} indicates that the r_i coordinate is missing in the basis function as shown and the channel index $\mu \equiv (n\lambda l)$.[23] The total $(N+1)$-electron wave function is now expanded in an explicitly antisymmetrized form as

$$\Psi^T(\vec{x}_1, \ldots, \vec{x}_{N+1}) = \sum_{SM\Lambda\mu} \Psi_{\mu}^{SM\Lambda}(\vec{x}_1, \ldots, \vec{x}_{N+1}), \quad (5)$$

and

$$\Psi_{\mu}^{SM\Lambda}(\vec{x}_1, \ldots, \vec{x}_{N+1}) = \sum_{i=1}^{N+1} \sum_{\mu'} (N+1)^{-1/2}(-1)^{i-1} r_i^{-1} \times F_{\mu',\mu}(r_i)\psi_{\mu'}^{SM\Lambda}(X^{-i}), \quad (6)$$

where $r^{-1}F_{\mu',\mu}(r)$ are to be determined by solving the scattering equation. In this paper we will not consider the *bound* $(N+1)$-electron states in the expansion of Eq. (5). Inclusion of such bound states allows for the possibility of electron capture into the target molecule,[24] and would be essential in the studies of resonance behaviors of excitation functions such as in Ref. 20. We seek the solution of the Schrödinger equation,

$$(H-E)\Psi^T(\vec{x}_1, \ldots, \vec{x}_{N+1}) = 0, \quad (7)$$

where the $(N+1)$-electron Hamiltonian H is

$$H = H_{\text{mol}} - \tfrac{1}{2}\nabla_{N+1}^2 + V(\vec{r}_1, \ldots, \vec{r}_{N+1}), \quad (8)$$

$$V(\vec{r}_1, \ldots, \vec{r}_{N+1}) = -Z(|\vec{r}_A - \vec{r}_{N+1}|^{-1} + |\vec{r}_B - \vec{r}_{N+1}|^{-1}) + \sum_{i=1}^{N} |\vec{r}_i - \vec{r}_{N+1}|^{-1}. \quad (9)$$

In lieu of Eq. (7) we apply the variational principle to the integral (a standard prescription here),

$$\delta \int d\vec{x}_1 \ldots d\vec{x}_{N+1} \Psi_{\mu}^{SM\Lambda *}(\vec{x}_1, \ldots, \vec{x}_{N+1}) \times (H-E)\Psi^T(\vec{x}_1, \ldots, \vec{x}_{N+1}) = 0, \quad (10)$$

with a subsidiary condition that the scattered-electron functions be orthogonal to all the relevant target one-electron orbitals ϕ_j. (Imposition of this orthogonality condition precludes the possibility of electron capture into those orbitals.) For electron-atom problems, because of the spherical symmetry of the target, this is equivalent to requiring orthogonality between the scattered radial functions $r^{-1}F_{\mu',\mu}$ and the target orbitals of the same l. This orthogonality relation offers a great deal of simplification to the scattering equations. For molecular systems, the requirement of $r^{-1}F_{\mu',\mu}$ being orthogonal to the relevant molecular orbitals would certainly ensure the orthogonality of the colliding-electron wave function to the target states, but the former is somewhat more stringent than the latter. However, in this work we adopt the former version in order to take advantage of the simplification in handling the exchange terms in the scattering equation, i.e.,[25]

$$\int \phi_j^*(n_j\lambda_j | \vec{r})[Y_{l',\Lambda-\lambda'}(\hat{r})r^{-1}F_{n'\lambda'l'}(r)]d\vec{r} = 0. \quad (11)$$

Upon expanding

$$\phi_j(n_j\lambda_j | \vec{r}) = \sum_l Y_{l\lambda_j}(\hat{r})\phi_{j,l}(n_j\lambda_j | r), \quad (12)$$

Eq. (11) becomes

$$\sum_l \delta_{l,l'}\delta_{\lambda_j,\Lambda-\lambda'} \int \phi_{j,l}(n_j\lambda_j | r)r^{-1}F_{n'\lambda'l'}(r)r^2 dr = 0, \quad (13)$$

for all molecular orbitals $\phi_j(n_j\lambda_j | r)$. This orthogonality condition may be treated by means of the Lagrange undetermined multipliers $M_{n_j\lambda_j l}$. This amounts to adding to Eq. (10) the following equation:

$$\delta \int \sum_j \sum_l \delta_{l,l'}\delta_{\lambda_j,\Lambda-\lambda'} M_{n_j\lambda_j l}\phi_{j,l}(n_j\lambda_j | r) \times r^{-1}F_{n'\lambda'l'}(r)r^2 dr = 0. \quad (14)$$

From Eqs. (10) and (14), we obtain the familiar set of integro-differential equations.

$$\left(\frac{d^2}{dr^2} - \frac{l'(l'+1)}{r^2} + k'^2\right)F_{\mu',\mu}(r) = 2\sum_{\mu''}[U_{\mu'\mu''}(r) + W_{\mu',\mu''}(r)]F_{\mu'',\mu}(r) + \sum_j \sum_l \delta_{l,l'}\delta_{\lambda_j,\Lambda-\lambda'} M_{n_j\lambda_j l}\phi_{j,l}(n_j\lambda_j | r), \quad (15)$$

where the direct (U) and exchange (W) potentials are

$$U_{\mu',\mu''}(r_{N+1}) = \int \psi_{\mu'}^{SM\Lambda *}(X^{-(N+1)})V(\vec{r}_1, \ldots, \vec{r}_{N+1}) \times \psi_{\mu''}^{SM\Lambda}(X^{-(N+1)})\, d\vec{r}_1 \ldots d\vec{r}_N\, d\hat{r}_{N+1}, \quad (16)$$

$$W_{\mu'\mu''}(r_{N+1})F_{\mu''\mu}(r_{N+1}) = -N\int \psi_{\mu'}^{SM\Lambda*}(X^{-N})r_N^{-1}F_{\mu''\mu}(r_N)\left|\vec{r}_N-\vec{r}_{N+1}\right|^{-1} \times \psi_{\mu''}^{SM\Lambda}(X^{-(N+1)})d\vec{r}_1\ldots d\vec{r}_N d\vec{r}_{N+1}, \quad (17)$$

and

$$k'^2 = 2(E-E_{n'\lambda'}). \quad (18)$$

We will not attempt to simplify Eqs. (16) and (17) until we come to a specific application. However, we point out here that these coupling potentials vanish between channels of differing parity.[26] Parity of a channel $n\lambda l$ associated with $n\lambda$ electronic state may be defined as $(-1)^l$ for "gerade" states ($\Sigma_g,\Pi_g,\ldots$), and $(-1)^{l+1}$ for "ungerade" states ($\Sigma_u,\Pi_u,\ldots$). As a result, the scattering equations separate into two sets according to even or odd parity just as in an electron-atom collision problem. The solutions $F_{\mu'\mu}(r)$ are subject to the boundary conditions,

$$F_{\mu'\mu}(r)\to 0 \quad \text{as } r\to 0,$$

$$F_{\mu'\mu}(r)\sim\frac{1}{k'^{1/2}}\left[\delta_{\mu'\mu}e^{-i[k'r-(1/2)l'\pi]} - e^{i[k'r-(1/2)l'\pi]}S_{\mu'\mu}^{SM\Lambda}\right] \text{ as } r\to\infty, \quad (19)$$

where $S_{\mu'\mu}$ is the scattering matrix. Following a similar analysis of Blatt and Biedenharn,[12] the scattering amplitude is

$$f^{SM\Lambda}(n\lambda ls\to n'\lambda' l's'|\hat{k},\hat{r}) = \frac{2\pi}{(kk')^{1/2}}i^{l-l'}Y_{l,\Lambda-\lambda}^*(\hat{k})Y_{l',\Lambda-\lambda'}(\hat{r})T_{\mu'\mu}^{SM\Lambda}, \quad (20)$$

where the transition matrix T is

$$T_{\mu'\mu}^{SM\Lambda} = \delta_{\mu'\mu} - S_{\mu'\mu}^{SM\Lambda}. \quad (21)$$

The differential cross section in $\hat{r}$ direction is

$$I(n\lambda s\to n'\lambda's'|\hat{k},\hat{r}) = \frac{4\pi^2}{k^2}\sum_S\frac{2S+1}{2(2s+1)} \times\sum_{\Lambda ll'}\left|Y_{l,\Lambda-\lambda}(\hat{k})Y_{l',\Lambda-\lambda'}(\hat{r})T_{n'\lambda'l',n\lambda l}^{SM\Lambda}\right|^2. \quad (22)$$

Integration over the scattered angle yields a total cross section for a given incident direction ($\hat{k}$). As stated before, we are to average the cross sections with respect to $\hat{k}$, i.e.,

$$Q(n\lambda s\to n'\lambda's') = \frac{1}{4\pi}\int d\hat{k}\,d\hat{r}\,I(n\lambda s\to n'\lambda's'|\hat{k},\hat{r}) = \frac{\pi}{k^2}\sum_S\frac{2S+1}{2(2s+1)}\sum_{\Lambda ll'}\left|T_{n'\lambda'l',n\lambda l}^{SM\Lambda}\right|^2. \quad (23)$$

For the purpose of later discussions, it is convenient to have cross sections expressed as

$$Q(n\lambda s\to n'\lambda's') = \sum_S\frac{2S+1}{2(2s+1)}\sum_{\Lambda=-\infty}^{\infty}\sum_{l=|\Lambda-\lambda|}^{\infty}\sum_{l'=|\Lambda-\lambda'|}^{\infty}Q^{SM\Lambda}(n\lambda sl\to n'\lambda's'l'), \quad (24)$$

with

$$Q^{SM\Lambda}(n\lambda sl\to n'\lambda's'l') = \frac{\pi}{k^2}\left|T_{n'\lambda'l',n\lambda l}^{SM\Lambda}\right|^2. \quad (25)$$

In accordance with the FC approximation, Eq. (23) is viewed as the cross section from any *one* vibrational level of $n\lambda s$ to *all* vibrational levels of the $n'\lambda's'$ state. Therefore, cross sections between a pair of vibrational levels are to be scaled by the appropriate Franck-Condon factor $q_{nv,n'v'}$, i.e.,

$$Q(n\lambda sv\to n'\lambda's'v') = q_{nv,n'v'}Q(n\lambda s\to n'\lambda's'), \quad (26)$$

$$q_{nv,n'v'} = \left|\int\chi_{n'v'}^*(R)\chi_{nv}(R)R^2dR\right|^2,$$

where $\chi_{nv}(R)$ is the vibrational wave function of the nv state.

It is worthwhile to draw the contrast between the electron-atom and electron-molecule systems. An obvious difference is that the electronic wave functions of a diatomic molecule are centered around two nuclei. This causes difficulty in computing the coupling potentials, which will be discussed in Sec. IV A. The other point of practical interest is the following: In an electron-atom collision, the scattering equations are diagonal in $\vec{L}=\vec{l}_a+\vec{l}$ and M_L ($\vec{l}_a$ and $\vec{l}$ being the angular momenta of the atom and scattered electron, respectively), and the cross sections are independent of M_L. Accordingly, the cross sections corresponding to Eq. (24) are (apart from the parity consideration) given by

$$Q^{\text{atom}}(nl_as\to n'l_a's') = \sum_S\frac{2S+1}{2(2s+1)}\sum_{L=0}^{\infty}\frac{2L+1}{(2l_a+1)}\sum_{l=|L-l_a|}^{L+l_a}\sum_{l'=|L-l_a'|}^{L+l_a'}Q^{LS}(nl_als\to n'l_a'l's'). \quad (27)$$

Thus, once the number of target states nl_a is decided on, one set of scattering equations corresponding to a given pair of L, M_L are solved at a time, yielding partial cross sections Q^{LS}. Further, for a given L, l and l' are restricted to a finite number of values as shown in Eq. (27). Strictly speaking, L runs from 0 to ∞. In practice, since the partial cross sections Q^{LS} diminish with increasing L for large L, the series in Eq. (27) may be terminated after summing a finite number of Q^{LS} for $L = 0, 1, \ldots, L_{\max}$. The point we like to emphasize here is that $L_{\max}$ is chosen—and may be increased later—according to the knowledge of partial cross sections Q^{LS} already calculated for $L \leq L_{\max}$.

However, for the electron excitation of molecules considered in this paper, only Λ is a good quantum number.[27] Thus the scattering equations for a given Λ would in principle contain an infinite number of channels corresponding to $l = |\Lambda - \lambda|$, $|\Lambda - \lambda| + 2, \ldots$ as shown in Eq. (24). Again, truncation of channels (with respect to l) is inevitable. However, in this case the truncation must be made before the scattering equations are solved. In other words, whether or not a sufficient number of channels were included in a calculation can be ascertained only after the calculation had already been completed. This is an additional burden in the calculation of molecular excitation. We will discuss this further in Sec. III.

III. APPLICATION TO ELECTRON-H_2 COLLISION

Within the theoretical framework outlined in Sec. II, we made a series of two-state close-coupling calculations by including the ground state $X\,^1\Sigma_g^+$ and each of the $B\,^1\Sigma_u^+$, $a\,^3\Sigma_g^+$, $b\,^3\Sigma_u^+$, $c\,^3\Pi_u$, and $e\,^3\Sigma_u^+$ states. With the number of electronic states thus limited to two, we must still decide how many partial waves (ll') are to be included in a calculation, as pointed out at the end of Sec. II. After some test calculations we found that for the singlet-triplet excitation it is quite adequate to include three partial waves or less per electronic state in the energy range (up to 40 eV) of incident electron considered here. However, in the case of excitation to the singlet state ($B\,^1\Sigma_u^+$), it appears that a very large number of partial waves would be required. Therefore we adopt the following practical scheme[18] to carry out the close-coupling calculations with a limited number of partial waves while maintaining sufficient degree of accuracy.

A. Special treatment for singlet-singlet excitation

Let us denote the close-coupling (CC) cross section of $X\,^1\Sigma_g^+ \rightarrow B\,^1\Sigma_u^+$ excitation by

$$Q^{(\mathrm{CC})}(B\,^1\Sigma_u^+) = \sum_{ll'} \sum_{\Lambda} Q^{(\mathrm{CC})\Lambda}(l,l') . \tag{28}$$

This is a shorthand version of Eq. (24) with $S = M = \frac{1}{2}$ and $s = s' = 0$. We assert here that for sufficiently large l, $l' > L$, $Q^{(\mathrm{CC})\Lambda}(l,l')$ approach the corresponding partial cross sections $Q^{(\mathrm{Born})\Lambda}(l,l')$ by the Born approximation. Barnes, Lane, and Lin[16] verify this in their work on electron-Na collisions with a qualitative physical reason behind it. Therefore we may calculate $Q^{(\mathrm{CC})\Lambda}(l,l')$ for $l, l' \leq L$, and substitute $Q^{(\mathrm{Born})\Lambda}(l,l')$ for $Q^{(\mathrm{CC})\Lambda}(l,l')$ for $(l,l') > L$, viz.,

$$\begin{aligned} Q^{(\mathrm{CC})}(B\,^1\Sigma_u^+) &\simeq \sum_{ll'}^{L} \sum_{\Lambda} Q^{(\mathrm{CC})\Lambda}(l,l') + \sum_{l'>L} \sum_{\Lambda} Q^{(\mathrm{Born})\Lambda}(l,l') \\ &= Q^{(\mathrm{Born})}_{(\mathrm{total})} + \sum_{ll'}^{L} \left(\sum_{\Lambda} [Q^{(\mathrm{CC})\Lambda}(l,l') - Q^{(\mathrm{Born})\Lambda}(l,l')] \right) . \end{aligned} \tag{29}$$

We will substantiate this claim later.

B. Coupling potentials

The electronic wave functions used in this work are as follows:

$$\begin{aligned} &\Phi(X\,^1\Sigma_g^+; s = m = 0) = [1\sigma_g\alpha(1)1\sigma_g\beta(2)] , \\ &\Phi(B\,^1\Sigma_u^+; s = m = 0) = \sqrt{\tfrac{1}{2}}\, \{[1\sigma_g\alpha(1)1\sigma_u\beta(2)] \\ &\qquad\qquad - [1\sigma_g\beta(1)1\sigma_u\alpha(2)]\} , \\ &\Phi(a\,^3\Sigma_g^+; s = 1, m = 0) = \sqrt{\tfrac{1}{2}}\, \{[1\sigma_g\alpha(1)2\sigma_g\beta(2)] \\ &\qquad\qquad + [1\sigma_g\beta(1)2\sigma_g\alpha(2)]\} , \\ &\Phi(a\,^3\Sigma_g^+; s = m = 1) = [1\sigma_g\alpha(1)2\sigma_g\alpha(2)] , \end{aligned} \tag{30}$$

and similarly for $b\,^3\Sigma_u^+$, $e\,^3\Sigma_u^+$, and $c\,^3\Pi_u$ ($\lambda = \pm 1$) states with $2\sigma_g$ replaced respectively by $1\sigma_u$, $2\sigma_u$, and $1\pi_u$ ($\lambda = \pm 1$) orbitals. Here, we used the brackets to represent the normalized determinants. The detailed form of the molecular orbitals will be given later. The threshold energies of these states are listed in Table I, which should be viewed in the context of the FC approximation. Let us con-

TABLE I. Threshold (vertical excitation) energies in eV.

$X\,^1\Sigma_g^+$	$B\,^1\Sigma_u^+$	$b\,^3\Sigma_u^+$	$a\,^3\Sigma_g^+$	$c\,^3\Pi_u$	$e\,^3\Sigma_u^+$
0.0	11.37	10.50	11.80	11.96	13.22

TABLE II. Coupling potentials for ($x\ ^1\Sigma_g^+, B\ ^1\Sigma_u^+$) system.

	$X\ ^1\Sigma_g^+$	$B\ ^1\Sigma_u^+$
$X\ ^1\Sigma_g^+$	$2(1\sigma_g, 1\sigma_g) + \{1\sigma_g, 1\sigma_g\}$	$\sqrt{2}(1\sigma_u, 1\sigma_g) + (1/\sqrt{2})\{1\sigma_u, 1\sigma_g\}$
$B\ ^1\Sigma_u^+$	$\sqrt{2}(1\sigma_g, 1\sigma_u) + (1/\sqrt{2})\{1\sigma_g, 1\sigma_u\}$	$(1\sigma_g, 1\sigma_g) + (1\sigma_u, 1\sigma_u)$ $\frac{1}{2}\{1\sigma_g, 1\sigma_g\} + \frac{1}{2}\{1\sigma_u, 1\sigma_u\}$

sider a process in which an incident electron ($s = m_s = \frac{1}{2}$) impinges upon an H_2 molecule in the ground state ($s = m_s = 0$). Consistent with this, we construct basis functions as in Eq. (4), which are spin eigenfunctions of $S = M = \frac{1}{2}$ with $N = 2$. For example, with the $X\ ^1\Sigma_g^+$ state we have

$$\psi^{SM\Lambda}_{X\lambda l s}(X^{-3}) = Y_{l,\Lambda-\lambda}(\hat{r}_3)\alpha(3)\Phi(X\ ^1\Sigma_g^+; s = m = 0)\,, \tag{31}$$

and likewise for the $B\ ^1\Sigma_u^+$ state. In the case of $a\ ^3\Sigma_g^+$ we write

$$\psi^{SM\Lambda}_{a\lambda l s}(X^{-3}) = Y_{l,\Lambda-\lambda}(\hat{r}_3)[\sqrt{\tfrac{2}{3}}\beta(3)\Phi(a\ ^3\Sigma_g^+; s = m = 1) - \sqrt{\tfrac{1}{3}}\alpha(3)\Phi(a\ ^3\Sigma_g^+; s = 1, m = 0)] \tag{32}$$

The basis functions associated with other triplet states are obtained similarly. With these explicit expressions [Eqs. (30)–(32)], the potentials [Eqs. (16),(17)] may be reduced to the following:

$$U_{\mu\mu'}(r) = \delta_{s,s'}[V^N_{n\lambda l s, n'\lambda' l' s'}(r) + V^e_{n\lambda l s, n'\lambda' l' s'}(r)]\,, \tag{33}$$

where

$$V^N_{n\lambda l s, n'\lambda' l' s'}(r) = -\delta_{(n\lambda),(n'\lambda')} \times \int d\hat{r}\, Y^*_{l,\Lambda-\lambda}(\hat{r}) Y_{l',\Lambda-\lambda'}(\hat{r}) \times [|\vec{r}_A - \vec{r}|^{-1} + |\vec{r}_B - \vec{r}|^{-1}]\,, \tag{34}$$

and

$$V^e_{n\lambda l s, n'\lambda' l' s'}(r) = \int d\hat{r}\, Y^*_{l,\Lambda-\lambda}(\hat{r}) Y_{l',\Lambda-\lambda'}(\hat{r}) \times \sum_j f_j \int \phi_j^*(\vec{r}')|\vec{r} - \vec{r}'|^{-1} \times \phi_j'(\vec{r}')\, d\vec{r}'\,. \tag{35}$$

The Kronecker delta in Eq. (33) restricts the direct-coupling potentials to those between channels belonging to electronic states of same spin, with the obvious consequence that a singlet-to-triplet excitation is achieved only through electron-exchange. The potential due to the nuclear charge V^N is diagonal in electronic states as shown in Eq. (34). The part due to the molecular electrons V^e is a sum of integrals involving one-electron molecular orbitals (MO) ϕ_j, ϕ_j' with numerical factors f_j. Analogous to this, we find

$$W_{\mu\mu'}(r)F_{\mu'\mu''}(r) = -\sum_j g_j \int \phi_j^*(\vec{r}')Y_{l',\Lambda-\lambda'}(\hat{r}')|\vec{r} - \vec{r}'|^{-1} \times \phi_j'(\vec{r})Y^*_{l,\Lambda-\lambda}(\hat{r})(rr')^{-1}F_{\mu'\mu''}(r')\, d\hat{r}\, d\vec{r}'\,. \tag{36}$$

For convenience we use shorthand notations:

$$(\phi_j', \phi_j) \equiv \int \phi_j^*(\vec{r}')|\vec{r} - \vec{r}'|^{-1}\phi_j'(\vec{r}')\, d\vec{r}'\,, \tag{37}$$

$$\{\phi_j', \phi_j\} \equiv \int \phi_j^*(\vec{r}')Y_{l',\Lambda-\lambda'}(\hat{r}')|\vec{r} - \vec{r}'|^{-1} \times \phi_j'(\vec{r})Y^*_{l,\Lambda-\lambda}(\hat{r})(rr')^{-1}F_{\mu'\mu''}(r')\, d\hat{r}\, d\vec{r}'\,. \tag{38}$$

We display in Tables II–IV the coupling potentials

TABLE III. Coupling potentials for ($X\ ^1\Sigma_g^+, a\ ^3\Sigma_g^+$) system.[a]

	$X\ ^1\Sigma_g^+$	$a\ ^3\Sigma_g^+$
$X\ ^1\Sigma_g^+$	$2(1\sigma_g, 1\sigma_g) + \{1\sigma_g, 1\sigma_g\}$	$\sqrt{\frac{3}{2}}\{2\sigma_g, 1\sigma_g\}$
$a\ ^3\Sigma_g^+$	$\sqrt{\frac{3}{2}}\{1\sigma_g, 2\sigma_g\}$	$(1\sigma_g, 1\sigma_g) + (2\sigma_g, 2\sigma_g)$ $-\frac{1}{2}\{1\sigma_g, 1\sigma_g\} - \frac{1}{2}\{2\sigma_g, 2\sigma_g\}$

[a]Tables for ($X\ ^1\Sigma_g^+, b\ ^3\Sigma_u^+$) and ($X\ ^1\Sigma_g^+, e\ ^3\Sigma_u^+$) systems are similarly obtained by substituting $1\sigma_u$ and $2\sigma_u$ orbitals respectively for the $2\sigma_g$ orbital.

TABLE IV. Coupling potentials for ($X\ ^1\Sigma_g^+$, $c\ ^3\Pi_u$) system.[a]

	$X\ ^1\Sigma_g^+$	$c\ ^3\Pi_u(\lambda=+1)$	$c\ ^3\Pi_u(\lambda=-1)$
$X\ ^1\Sigma_g^+$	$2(1\sigma_g, 1\sigma_g) + \{1\sigma_g, 1\sigma_g\}$	$\sqrt{\frac{3}{2}}\{1\pi_u^+, 1\sigma_g\}$	$\sqrt{\frac{3}{2}}\{1\pi_u^-, 1\sigma_g\}$
$c\ ^3\Pi_u(\lambda=+1)$	$\sqrt{\frac{3}{2}}\{1\sigma_g, 1\pi_u^+\}$	$(1\sigma_g, 1\sigma_g) + (1\pi_u^+, 1\pi_u^+)$ $-\frac{1}{2}\{1\sigma_g, 1\sigma_g\} - \frac{1}{2}\{1\pi_u^+, 1\pi_u^+\}$	$(1\pi_u^-, 1\pi_u^+) - \frac{1}{2}\{1\pi_u^-, 1\pi_u^+\}$
$c\ ^3\Pi_u(\lambda=-1)$	$\sqrt{\frac{3}{2}}\{1\sigma_g, 1\pi_u^-\}$	$(1\pi_u^+, 1\pi_u^-) - \frac{1}{2}\{1\pi_u^+, 1\pi_u^-\}$	$(1\sigma_g, 1\sigma_g) + (1\pi_u^-, 1\pi_u^-)$ $-\frac{1}{2}\{1\sigma_g, 1\sigma_g\} - \frac{1}{2}\{1\pi_u^-, 1\pi_u^-\}$

[a] One-electron orbitals π^+ and π^- refer to $\pi(\lambda=+1)$ and $\pi(\lambda=-1)$, respectively.

between channels with respect to the electronic states to which they belong.

In order to express these potentials more explicitly we use the following well-known expansions, with the origin of the coordinate system chosen at the center of homonuclear diatomic molecule as shown in Fig. 1. That is,

$$|\vec{r}_A - \vec{r}|^{-1} = \frac{1}{R_>}\sum_K \left(\frac{4\pi}{2K+1}\right)^{1/2}\left(\frac{R_<}{R_>}\right)^K Y_{K,0}(\hat{r}), \quad (39)$$

$$|\vec{r}_B - \vec{r}|^{-1} = \frac{1}{R_>}\sum_K (-1)^K\left(\frac{4\pi}{2K+1}\right)^{1/2}\left(\frac{R_<}{R_>}\right)^K Y_{K,0}(\hat{r}), \quad (40)$$

$$|\vec{r} - \vec{r}'|^{-1} = \frac{1}{r_>}\sum_K \left(\frac{4\pi}{2K+1}\right)\left(\frac{r_<}{r_>}\right)^K \sum_m Y^*_{K,m}(\hat{r}')Y_{K,m}(\hat{r}), \quad (41)$$

where $R_>$ and $R_<$ stand for the greater or lesser of r and $\frac{1}{2}R$, and $r_>$ and $r_<$ for greater or lesser of r and r'. With these expansions we find

$$V^N_{n\lambda l s, n'\lambda' l' s'}(r) = -\delta_{(n\lambda),(n'\lambda')}\left(\frac{2}{R_>}\right) \times \sum_{\substack{K=|l-l'| \\ (K=\text{even})}}^{l+l'} c^K(l'\Lambda-\lambda', l\Lambda-\lambda)\left(\frac{R_<}{R_>}\right)^K, \quad (42)$$

$$V^e_{n\lambda l s, n'l'l's'}(r) = \sum_j f_j \sum_{K=|l-l'|}^{l+l'} c^K(l'\Lambda-\lambda', l\Lambda-\lambda) \times y_K(\phi_j, \phi'_j|r), \quad (43)$$

where we used the notation of Condon and Shortley,[28] i.e.,

$$c^K(l'm', lm) = \left(\frac{4\pi}{2K+1}\right)^{1/2}\int d\hat{r}\, Y^*_{lm}(r)Y_{K,m-m'} \times(r)Y_{l'm'}(\hat{r}), \quad (44)$$

and the y_K function is

$$y_K(\phi_j, \phi'_j|r) = (-1)^{\lambda'_j-\lambda_j}\left(\frac{4\pi}{2K+1}\right)^{1/2}\int \phi^*_j(n_j,\lambda_j|\vec{r}')Y_{K,\lambda_j-\lambda'_j}(\hat{r}')\left(\frac{1}{r_>}\right)\left(\frac{r_<}{r_>}\right)^K \phi'_j(n'_j\lambda'_j|\vec{r}')\,d\vec{r}'$$

$$= (-1)^{\lambda'_j-\lambda_j}\left(\frac{4\pi}{2K+1}\right)^{1/2}\left[\left(r^{-K-1}\int_0^r r'^K r'^2\,d\hat{r}' + r^K\int_r^\infty r'^{-K-1}r'^2\,dr'\right) \times\left(\int d\hat{r}'\,\phi^*_j(n_j\lambda_j|\vec{r}')Y_{K,\lambda_j-\lambda'_j}(\hat{r}')\,\phi'_j(n'_j\lambda'_j|\vec{r}')\right)\right], \quad (45)$$

where λ_j is the angular momentum along the molecular axis of a *molecular orbital* ϕ_j. Similarly,

$$W_{\mu\mu'}(r)F_{\mu'\mu''}(r) = -\sum_j g_j \sum_{K,g}\left(\frac{4\pi}{2K+1}\right) r\int d\hat{r}\, Y^*_{Kg}(\hat{r})Y^*_{l,\Lambda-\lambda}(\hat{r})\phi'_j(\vec{r}) \times\left[\left(r^{-K-1}\int_0^r r'^K F_{\mu'\mu''}(r')\,dr' + r^K\int_r^\infty r'^{-K-1}F_{\mu'\mu''}(r')\,dr'\right) \times r'\int d\hat{r}'\,Y_{Kg}(\hat{r}')Y_{l',\Lambda-\lambda'}(\hat{r}')\phi^*_j(\vec{r}')\right]. \quad (46)$$

To simplify this we use the relation

$$Y_{l_1m_1}(\hat{r})Y_{l_2m_2}(\hat{r}) = \sum_{L=|l_1-l_2|}^{l_1+l_2} \left(\frac{(2l_1+1)(2l_2+1)}{4\pi(2L+1)}\right)^{1/2} \times C(l_1l_2m_1m_2|LM=m_1+m_2) \times C(l_1l_200|L0)Y_{LM}(\hat{r}), \quad (47)$$

and define a function Z_K, viz.,

$$Z_K(\phi_j lm|r) = \left(\frac{4\pi}{2K+1}\right)^{1/2} r \int d\hat{r}\, Y_{Kg}(\hat{r})Y_{lm}(\hat{r})\phi_j^*(\vec{r}) = r \sum_{L=|K-l|}^{K+l} \left(\frac{2l+1}{2L+1}\right)^{1/2} C(Klgm|LM) \times C(Kl00|L0) \times \int d\hat{r}\, Y_{LM}(\hat{r})\phi_j^*(n_j\lambda_j|\vec{r}). \quad (48)$$

The last integral in the above equation restricts $M=\lambda_j$, which in turn sets $g=\lambda_j - m$ so that the summation over g is merely formal in Eq. (46). Combining Eqs. (47) and (48) into (46), we find

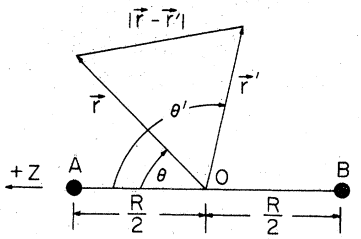

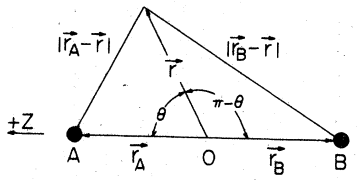

FIG. 1. Coordinate system showing the expansions of $|\vec{r}-\vec{r}'|^{-1}$, $|\vec{r}_A-\vec{r}|^{-1}$, and $|\vec{r}_B-\vec{r}|^{-1}$.

$$W_{\mu\mu'}(r)F_{\mu'\mu''}(r) = -\sum_j g_j \sum_K Z_K^*(\phi_j' l\Lambda-\lambda|r)\left[\left(r^{-K-1}\int_0^r r'^K F_{\mu'\mu''}(r')\,dr' + r^K\int_r^\infty r'^{-K-1}F_{\mu'\mu''}(r')\,dr'\right)Z_K(\phi_j l'\Lambda-\lambda'|r')\right]. \quad (49)$$

We note that the parameter K in Eqs. (42) and (43) and L in Eq. (48) are limited to a finite number of values so that those series [Eqs. (42), (43), and (48)] can be summed without any omission as indeed done in this work. The exception to this occurs in Eq. (49) with regard to K, where K has no upper limit. As a practical matter this infinite series must be truncated, and we found it sufficient to retain the three leading terms in this work.

IV. METHOD OF COMPUTATION

In the usual approach of expressing the molecular orbitals (MO) by linear combinations of atomic orbitals (LCAO), the molecular wave functions are centered around the two nuclei. The greatest (if not the only) difficulty with an electron-molecule calculation arises from this two-center nature of molecular function, the consequence of which needs no elaboration here. In this section we develop a computational technique suitable for the potentials by exploiting the advantages offered by the Gaussian-type orbitals (GTO).

To begin with, we define Gaussian functions centered at A and B with exponents a, b (see Fig. 2),

$$G(a,A) \equiv \exp\{-a[(x-A_x)^2+(y-A_y)^2+(z-A_z)^2]\} = \exp[-a(\tfrac{1}{4}R^2+r^2+Rr\cos\theta)] \quad (50)$$

$$G(b,B) = \exp[-b(\tfrac{1}{4}R^2+r^2-Rr\cos\theta)]. \quad (51)$$

The Gaussians shown above are known as s type, from which p_z-, p_x-, and p_y-type GTO can be de-

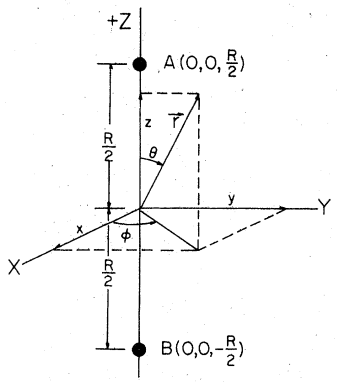

FIG. 2. Gaussian-type orbitals in the Cartesian and spherical coordinate systems.

rived, i.e.,

$$G_{p_z}(a,A) = (z - A_z)G(a,A) = (r\cos\theta - \tfrac{1}{2}R)G(a,A),$$
$$G_{p_x}(a,A) = (x - A_x)G(a,A) = r\sin\theta\cos\phi G(a,A), \quad \text{etc.} \tag{52}$$

Crucial to our computational procedure is the fact that the exponent in Eq. (50) is *rational*; in contrast, for the Slater-type orbitals (STO) the exponent would be *irrational*. In terms of these Gaussian functions, the one-electron molecular orbitals appearing in Eq. (30) are expressed as

$$\phi_{\sigma_g,\sigma_u} = \sum_{i=1}^{6} c_i[G(a_i,A) \pm G(a_i,B)] + \sum_{j=7}^{10} c_j[(r\cos\theta - \tfrac{1}{2}R)G(a_j,A) \mp (r\cos\theta + \tfrac{1}{2}R)G(a_j,B)], \tag{53}$$

with σ_g and σ_u taking the upper and lower signs, respectively, and

$$\phi_{\pi_u} = e^{\pm i\phi}\sum_{j=7}^{10} c_j r\sin\theta[G(a_j,A) + G(a_j,B)]. \tag{54}$$

The expansion coefficients c's are determined by the self-consistent-field (SCF) calculations for each of the $X\,^1\Sigma_g^+$, $B\,^1\Sigma_u^+$, $a\,^3\Sigma_g^+$, $b\,^3\Sigma_u^+$, $c\,^3\Pi_u$, and $e\,^3\Sigma_u^+$ states at $R = 0.74$ Å corresponding to the equilibrium separation of the ground state ($X\,^1\Sigma_g^+$). These coefficients are listed in Table V along with the corresponding exponents of six s-type and four p-type Gaussians.[29] The general procedure of SCF calculation is discussed in the literature.[30] In case of $(1\sigma_g)(2\sigma_u)e\,^3\Sigma_u^+$ which is the second lowest state of this symmetry, the SCF procedure is applied to the second lowest root of the secular equation; the $2\sigma_u$ orbital so obtained is found to be orthogonal to the $1\sigma_u$ orbital of the $(1\sigma_g)(1\sigma_u)b\,^3\Sigma_u^+$ state. In all cases the orbital coefficients are converged within 10^{-5}.

A. Coupling potentials

With a substitution of Eqs. (53) and (54), reduction of the last integral in Eq. (48) becomes possible. For example, we have

$$\int d\hat{r}\, Y_{LM}(\hat{r})\phi^*_{\pi_u}(\lambda_j = 1\,|\,\vec{r}) = \frac{1}{\sqrt{2\pi}}\int_0^{2\pi} d\phi\, e^{i(M-1)\phi}\sum_i c_i \exp[-a(\tfrac{1}{4}R^2 + r^2)] \times \int_0^{\pi}\sin\theta\, d\theta\,[\Theta_{LM}(\cos\theta,\sin\theta)r\sin\theta][\exp(-a_i Rr\cos\theta) + \exp(a_i Rr\cos\theta)], \tag{55}$$

and similarly with other MO. Thus, a typical θ integral has the form of

$$\int_0^{\pi}\sin\theta\, d\theta\,\Theta_{LM}(\cos\theta,\sin\theta)f(\cos\theta,\sin\theta)\exp(\gamma r\cos\theta), \qquad \gamma = \pm aR. \tag{56}$$

In practice the products $\Theta_{LM}(\cos\theta,\sin\theta)$ $\times f(\cos\theta,\sin\theta)$ always turn out to be an even sine function ($\sin^{2n}\theta$) so that we have to deal only with the following integral:

$$\int_0^{\pi}\sin\theta\, d\theta(\cos^n\theta)\, e^{x\cos\theta} = P_n(x)\, e^{-x} + Q_n(x)e^{x}, \tag{57}$$

where

TABLE V. Expansion coefficients of molecular orbitals as defined in Eqs. (53) and (54).

	Exponents	$1\sigma_g(X\,^1\Sigma_g^+)$	$1\sigma_u(B\,^1\Sigma_u^+)$	$1\sigma_u(b\,^3\Sigma_u^+)$	$2\sigma_u(e\,^3\Sigma_u^+)$	$2\sigma_g(a\,^3\Sigma_g^+)$	$1\pi_u(c\,^3\Pi_u)$
				s type			
1	0.082 217	0.008 161	0.014 707	0.072 015	0.085 134	-0.079 538	
2	0.224 660	0.056 787	0.012 820	0.114 357	-0.041 434	0.097 826	
3	0.673 320	0.109 047	0.013 728	0.097 461	-0.047 528	0.023 497	
4	2.346 48	0.099 505	0.017 342	0.065 106	-0.029 563	0.047 893	
5	10.246 5	0.065 448	0.012 806	0.040 253	-0.018 133	0.017 078	
6	68.160 0	0.035 669	0.006 979	0.021 938	-0.009 883	0.009 308	
				p type			
7	0.020 185	0.000 047	0.002 002	0.000 336	0.007 021	0.013 628	0.001 276
8	0.055 713	-0.000 204	0.010 115	0.004 223	-0.013 251	-0.032 689	0.007 440
9	0.174 211	-0.001 571	0.014 515	0.009 789	-0.019 582	0.012 642	0.014 973
10	0.733 825	-0.021 730	0.016 108	0.025 107	-0.006 282	-0.032 281	0.022 637

$$P_n(x) = (-1)^{n+1}\sum_{m=0}^{n} \frac{n!}{(n-m)!\,x^{m+1}}$$

and

$$Q_n(x) = (-1)^n P_n(-x). \tag{58}$$

The angular integrations for the y_K function in Eq. (45) are performed in a similar manner; the only difference is that there are two MO in the integrand so that the number of terms is increased. However, the form remains the same.

Thus, with the angular integration completed, r integration is carried out numerically by Simpson's rule for y_K function in Eq. (45). From this V^e are assembled in accordance with Eq. (43), and subsequently by combining V^e and V^N, we obtain $U_{\mu\mu'}(r)$ in Eq. (33) in a tabular form from $r = 0$ to $31a_0$, beyond which $U_{\mu\mu'}(r)$ are fitted to a two-term asymptotic form, i.e.,

$$U_{\mu\mu'}(r) = a/r^k + b/r^{k+2}. \tag{59}$$

This curve fitting is based on 50 data points between $r = 31$ and $41a_0$ with a maximum error of 0.1% for the worst case. For numerical integration we start with a mesh size $\delta r = 0.0125a_0$ and double it after every 80 quadrature points until $\delta r = 0.1a_0$ is reached as shown in Table VI. This quadrature scheme is common to all numerical procedures, i.e., with y_K, Z_K, and the scattered wave F_{ij} of Sec. IV B, so that the potentials are fed into the scattering equation as they were calculated without further manipulations, except the asymptotic fitting of $U_{\mu\mu'}$ described above.

Similarly, the Z_K functions are tabulated as prescribed by Eq. (48) from $r = 0$ to a suitable cutoff value r_{cut}, beyond which the exchange potentials are set to zero. The effective range of exchange is expected to be roughly the extent of the molecular orbitals. In our test calculations we found no appreciable difference (less than 0.2%) in cross sections when we used $r_{\text{cut}} = 20$, 25, and $31a_0$. For the sake of safety, however, we settled on $r_{\text{cut}} = 25a_0$, accepting the waste of "overkill."

To ascertain the effect of truncation in the summation over K of Eq. (49), we performed test calculations with the $b\,^3\Sigma_u^+$ state at $E = 15$ eV by retaining one, three, and five Z_K terms in Eq. (49). With five Z_K terms, the partial cross sections for $\Lambda = 0$ are 0.018 07, 0.1204×10^{-3}, $0.1473 \times 10^{-6} a_0^2$, respectively, for $(l, l') = (0, 1)$, (2, 3), and (4, 5) as shown in Table VII. The corresponding partial cross sections with three Z_K terms are 0.018 10, 0.1210×10^{-3}, and 0.1141×10^{-6}, and with one term. they are 0.018 29, 0.1816×10^{-4}, and 0.2725×10^{-10}. The difference between the three- and five-term results is quite negligible with respect to both the partial cross sections and the total cross section. With regard to the one-term calculation, the larger discrepancy in the (2, 3) and (4, 5) partial cross sections over the (0, 1) may be understood in the following way. Namely, the last integral of Eq. (48) is nothing but a decomposition of MO ϕ_j by angular momentum, i.e.,

$$\phi_{j,L}(n_j\lambda_j|r) = \int d\hat{r}\, Y_{L,M}(\hat{r})\phi_j^*(n_j\lambda_j|\vec{r}). \tag{60}$$

For the MO's of H_2 considered here, we find that the largest concentrations are in $\phi_{1\sigma_g,0}$, $\phi_{1\sigma_u,1}$, etc., over other higher-angular-momentum components. These large components will enter into the summation of Eq. (48) only if $K = l$, $l \pm 1$ so that, viewed from this point, $Z_{K=l}$ and $Z_{K=l\pm1}$ are important terms. In the above example with only the $Z_{K=0}$ term, other important terms $Z_{K=2}$ and $Z_{K=4}$ are not taken into account, and this omission may explain the unsatisfactory results for $(l, l') = (2, 3)$ and (4, 5). Since these higher partial waves contribute much less to the total cross section than the lower ones, the

TABLE VI. Step size of integration regions[a] in a_0.

r_A	δr	r_B
0.0125	0.0125	1.0
1.0125	0.025	3.0
3.05	0.05	7.0
7.1	0.1	...

[a] r_A and r_B are the starting and final points of a region.

TABLE VII. Partial cross sections[a] $Q^{\Lambda=0}(l, l')$ in a_0^2 defined as in Eq. (25) for the $b\,^3\Sigma_u^+$ state at $E = 15$ eV.

l \ l'	0	1	2	3	4	5
0		0.181(-1)		0.779(-4)		0.181(-7)
1	0.413(0)		0.129(-1)		0.913(-5)	
2		0.583(-2)		0.120(-3)		0.180(-7)
3	0.319(-2)		0.735(-3)		0.317(-5)	
4		0.138(-4)		0.368(-4)		0.147(-6)
5	0.768(-4)		0.597(-5)		0.305(-5)	

[a] Numbers in parentheses indicate powers of 10.

net effect on the total cross section is merely 0.5% in this case even with only one Z_K term. We expect some minor fluctuations in this discrepancy (0.5%) as we change the incident-electron energy, and consider different electronic states. Therefore, in order to leave ample margin of safety to cover such variations, we decided to retain three leading, nonvanishing Z_K terms in Eq. (49) (e.g., $K=0,2,4$; $1,3,5$; or $2,4,6$, etc.) with $K \leq 9$ in all succeeding calculations presented in this paper.

B. Scattering equations

For the purpose of discussion here, we rewrite the integro-differential equations in Eq. (15) as follows:

$$\left(\frac{d^2}{dr^2} - \frac{l_i(l_i+1)}{r^2} + k_i^2\right) F_{ij}(r) = 2\sum_n [U_{in}(r) + W_{in}(r)] F_{nj}(r) + \sum_{J(\text{orbital})} \sum_{l(J)} \delta_{l,l_i}\delta_{\lambda_J,(\Lambda-\lambda_i)} M^{ij}_{J\lambda_J l} \phi_{J,l}(n_J\lambda_J|r), \tag{61}$$

where we used i,j for the scattering and incident channels, respectively. The summation J is over the molecular orbitals, and $l(J)$ covers even or odd values as dictated by the orbital $(J\lambda_J)$.

Once the $U(r)$, $W(r)$, and $\phi_{J,l}(r)$ are made available, the procedure of solution becomes quite analogous to atomic case. We solve this set of integro-differential equations by the noniterative integral equation method (NIEM).[15] Here, we give just a brief description of NIEM as applied to our problem, while the readers are referred to the paper by Smith and Henry[15] for details. We expect two sets of arbitrary constants which are to be determined by the boundary conditions. For the moment we look for the solutions $\psi_{ij}(r)$ of Eq. (61) without regard to boundary conditions, in place of $F_{ij}(r)$, which satisfy the boundary conditions. By means of the Green's-function technique, the solution can be expressed in an integral representation, i.e.,

$$\psi_{ij}(r) = \delta_{ij} G_i^{(1)}(k_i r) + 2\int_0^r dx\, G_i^{(2,1)}(r|x) \times \left\{ \sum_n U_{in}(x)\psi_{nj}(x) - \sum_n \sum_{p(in)} g_p \sum_K \left[Z_K(\phi^*_{p(n)} l_n \Lambda - \lambda_n | x) \times \left(x^{-K-1}\int_0^x y^K dy - x^K \int_0^x y^{-K-1} dy + x^K \int_0^\infty y^{-K-1} dy \right) \times Z_K(\phi_{p(i)} l_i \Lambda - \lambda_i | y)\psi_{nj}(y) \right] + \frac{1}{2}\sum_J \sum_{l(J)} \delta_{l,l_i}\delta_{\lambda_J,(\Lambda-\lambda_i)} M^{ij}_{J\lambda_J l} \phi_{J,l}(n_J\lambda_J|x) \right\}, \tag{62}$$

with

$$\begin{aligned} G_i^{(1)}(k_i r) &= k_i^{1/2} r j_{l_i}(k_i r), \\ G_i^{(2)}(k_i r) &= k_i^{1/2} r y_{l_i}(k_i r), \\ G_i^{(2,1)}(r|x) &= G_i^{(2)}(k_i r) G^{(1)}(k_i x) - G_i^{(1)}(k_i r) G_i^{(2)}(k_i x), \end{aligned} \tag{63}$$

where j_l and y_l are the spherical Bessel functions of the first and second kind, respectively. In Eq. (62) the summation $\sum_{p(in)}$ indicates the pair of MO $\phi_{p(n)}$ and $\phi_{p(i)}$ appearing in the two Z_K functions are dictated by the electronic states to which channels i and n belong. Equation (62) above corresponds to Eq. (12) of the paper by Smith and Henry. As they point out, the right side of Eq. (62) is known except the Lagrange multiplier M and the term

$$\int_0^\infty y^{-K-1} Z_K(\phi_{p(i)} l_i \Lambda - \lambda_i | y)\psi_{nj}(y)\, dy. \tag{64}$$

Since Eq. (61) is linear in ψ_{ij}, it is possible to treat these unknown terms as as inhomogeneity, and seek the complete solutions as appropriate linear combinations of the homogeneous and particular solutions. There is no point in attempting to reproduce their elegant treatment[15] here. We might note in passing that with K and $p(in)$ each taking three distinct values and nine channels, this amounts to in excess of 80 inhomogeneities including the orthogonality terms. However, all particular integrals as well as homogeneous solutions are processed simultaneously in the actual computation.

From the solutions $\psi_{ij}(r)$, the scattering matrix, may be determined as follows. For large distance

r, we may write

$$\psi_{ij}(r) \sim k_i^{-1/2}[\sin(k_i r - \tfrac{1}{2} l_i \pi) A_{ij} + \cos(k_i r - \tfrac{1}{2} l_i \pi) B_{ij}], \quad (65)$$

where we used the asymptotic form of the spherical Bessel functions j_l and y_l, and $\underline{A}$ and $\underline{B}$ are constant matrices to be determined. On the other hand the required asymptotic form is

$$F_{ij}(r) \sim k_i^{-1/2}[\sin(k_i r - \tfrac{1}{2} l_i \pi) \delta_{ij} + \cos(k_i r - \tfrac{1}{2} l_i \pi) R_{ij}]. \quad (66)$$

Therefore,

$$\underline{R} = \underline{B}\underline{A}^{-1}, \quad (67)$$

and

$$\underline{S} = (\underline{1} + i\underline{R})(\underline{1} - i\underline{R})^{-1}. \quad (68)$$

$\underline{A}$ and $\underline{B}$ matrices are determined numerically by matching $\psi_{ij}(r)$ at two adjacent points r_M and $r_M + \delta r$, that is, by setting up two simultaneous matrix equations for the two unknown matrices $\underline{A}$ and $\underline{B}$. In practice we chose $r_M = 31$ and $45a_0$ for the triplet cases, and $r_M = 45$, 55, and $65a_0$ for the $B\,^1\Sigma_u^+$ state to observe the proper convergence of the $\underline{R}$ matrix.

V. RESULTS AND DISCUSSION

We present the cross sections of the triplet states and the $B\,^1\Sigma_u^+$ state separately, as the two cases differ in treatment as well as in the energy range of interest.

A. Excitation to triplet states

The cross sections of the triplet states have been calculated by including partial waves $ll' \leq 5$, and $\Lambda = 0, 1, 2, 3$ at several incident-electron energies. Typical breakdown of cross sections by ll' at two different energies are shown in Tables VII and VIII. First, we note that the partial cross sections $Q^\Lambda(l, l')$ are much larger when $\Delta l = (l - l') = \pm 1$ than others. This is reminiscent of the dipole-selection rule applied to atomic excitation, in which cross sections are again found to be largest when $\Delta l = \pm 1$. Next, for a given sequence of Δl, $Q^\Lambda(l, l')$ decreases with increasing ll', although the effectiveness of large partial waves lingers on longer at high (40 eV) energy. There is no surprise here; the present results merely conform to the long-held view that only the low partial waves are effective at low incident-electron energies. In Table IX we show the breakdown of cross sections in terms of Λ, i.e.,

$$Q^\Lambda = \sum_{ll'} Q^\Lambda(l, l'). \quad (69)$$

Since $Q^{\Lambda=\pm n}$ are identical there is no need to repeat calculations with negative values of Λ. The decreasing trend of Q^Λ with increasing Λ is assured by the foregoing discussion as the low partial waves $Y_{l,\Lambda-\lambda}$ are eliminated with increasing Λ. Overall, it is evident from these tables that we have included sufficient number of partial waves even at the highest energy (40 eV) considered in this paper. We found a similar pattern in the partial cross sections with other triplet states. The total cross sections of the four triplet states are presented in Table X. We also included in this table cross sections by other theoretical calculations for comparison. There are some unexpected features as well as predictable ones in the excitation functions of these states. We now discuss these points as we compare the present close-coupling (CC) results with other theoretical calculations.

1. $b\,^3\Sigma_u^+$ and $e\,^3\Sigma_u^+$

The lowest excited state $b\,^3\Sigma_u^+$ is a repulsive state, which dissociates into two H(1s) atoms. The cross sections of this state are shown in Fig. 3. We have previously calculated these cross sections by using the Born-Rudge approximation[3]; they are included in Fig. 3 for comparison. The wave functions used there[3] are identical to those employed in the present work. These Born-Rudge (BR) cross sections are in essential agreement with the earlier calculation of similar nature by Cartwright and Kuppermann.[4] A dif-

TABLE VIII. Partial cross sections[a] $Q^{\Lambda=0}(l, l')$ in a_0^2 defined as in Eq. (25) for the $b\,^3\Sigma_u^+$ state at $E = 40$ eV.

l/l'	1	2	3	4	5
1		0.250(-2)		0.448(-5)	
2	0.475(-1)		0.244(-2)		0.308(-5)
3		0.102(-1)		0.481(-3)	
4	0.278(-4)		0.145(-2)		0.675(-4)
5		0.372(-5)		0.192(-3)	

[a] Numbers in parentheses indicate powers of 10.

TABLE IX. Partial cross sections $Q^\Lambda(b\,^3\Sigma_u^+)$ in a_0^2 defined as in Eq. (69) at $E = 15$ and 40 eV.

	Q^Λ	
Λ	$E = 15$ eV	$E = 40$ eV
0	0.454 019	0.077 405
1	0.271 013	0.064 906
2	0.002 737	0.006 672
3	0.000 038	0.000 721
Sum[a]	1.001 595	0.222 003

[a] $Q^{-\Lambda} = Q^{+\Lambda}$ $(\Lambda \neq 0)$ are included in the sum.

TABLE X. Total cross sections of triplet states in units of 10^{-17} cm^2.

Energy	$b\,^3\Sigma_u^+$			$e\,^3\Sigma_u^+$		$a\,^3\Sigma_g^+$			$c\,^3\Pi_u$	
(eV)	CC[a]	BR[b]	DW-RPA[c]	CC	BR	CC	BR	DW-RPA	CC	BR
13	2.19	4.47	8.24			0.269	1.07	0.571	4.63	1.96
14	2.56	4.41	9.23	1.285	0.330					
15	2.80	4.18	8.89	0.914	0.417	0.889	1.22	1.18	5.63	1.98
16	2.84	3.88	8.44					1.35		
17.5	2.81	3.41		0.620	0.421	0.715	1.06			
20	2.53	2.69	5.49	0.500	0.357	0.552	0.854	1.31	3.44	1.19
25	1.82	1.70		0.301	0.234	0.364	0.534		1.95	0.702
30	1.26	1.10		0.192	0.152	0.268	0.342		1.10	0.433
40	0.622	0.525		0.0902	0.0717	0.135	0.160		0.410	0.196

[a] Close coupling of this work.
[b] Born-Rudge approximation of Ref. 3.
[c] Distorted-wave with random-phase approximation of Ref. 11.

ference of about 20% in magnitude was attributed to the usage of different wave functions. Comparison of the present CC and the BR calculations shows that the former gives an appreciably broader excitation function and much smaller (~30%) cross sections below 20 eV. However, these two sets are in good agreement above 20 eV. We will not discuss the Born-type calculations of still earlier days[7,8] as the works described in Refs. 3 and 4 are representative of the Born-type calculations. Recently, Rescigno *et al.*[11] calculated

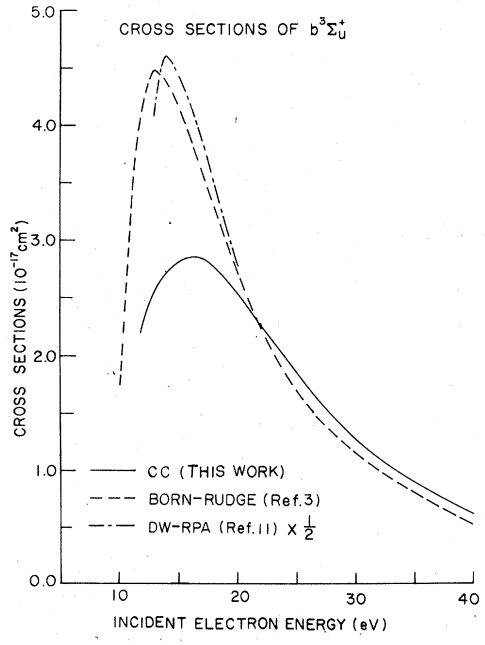

FIG. 3. Excitation cross sections of the $b\,^3\Sigma_u^+$ state calculated by means of (i) the close coupling (solid line) of this work; (ii) the Born-Rudge approximation (uniform dashed line) in Ref. 3; (iii) DW-RPA reduced to one-half (long-short dashed line) in Ref. 11.

cross sections of the $b\,^3\Sigma_u^+$ state by means of the distorted-wave approximation with random-phase approximation (DW-RPA) to compute the inelastic transition density. Their results are shown in Table X and also in Fig. 3. (In this figure the magnitude of their cross sections are reduced by a factor of 2). These authors[11] attempt to account for the distortion of the incident electron by means of the Coulomb and exchange operators for the molecule in the ground state. The same operators are used for the distortion of the scattered electron instead of the operators appropriate for the excited state. They justify this procedure based on the previous application of DW-RPA to electron-atom cases.[31] Besides this point, it is difficult to assess to what extent the static distortion in DW-RPA can represent the dynamic process. At any rate, their excitation function is rather similar to the BR calculation cited above, except the magnitude is about twice as large.

In drastic contrast to the $b\,^3\Sigma_u^+$ state, the excitation function of the $e\,^3\Sigma_u^+$ state shows an extremely sharp peak as shown in Fig. 4, even though these two states are of the same symmetry type. The cross section at 14 eV is considerably larger than that at 15 eV, but we did not attempt to locate the maximum. Compared with these CC results, the BR cross sections[3] are much smaller (factor of 4) near the threshold, but the difference becomes smaller at high incident energy (~20% at 40 eV).

The large difference in shape between the excitation functions of $b\,^3\Sigma_u^+$ and $e\,^3\Sigma_u^+$ found here, which is not revealed in the Born-Rudge calculation, is somewhat puzzling. One possible explanation is as follows: A singlet-triplet excitation involves an exchange between the colliding electron and a molecular electron. Its cross sections decrease drastically with energy if the colliding electron is found in the vicinity of the target for

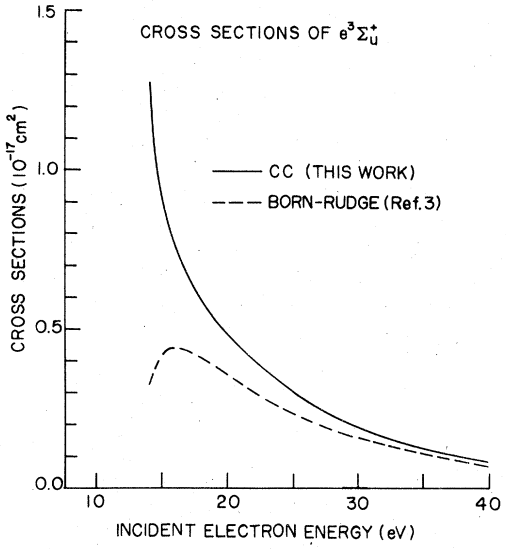

FIG. 4. Excitation cross sections of the $e\,^3\Sigma_u^+$ state calculated by means of (i) close coupling (solid line) of this work; (ii) the Born-Rudge approximation (dashed line) in Ref. 3.

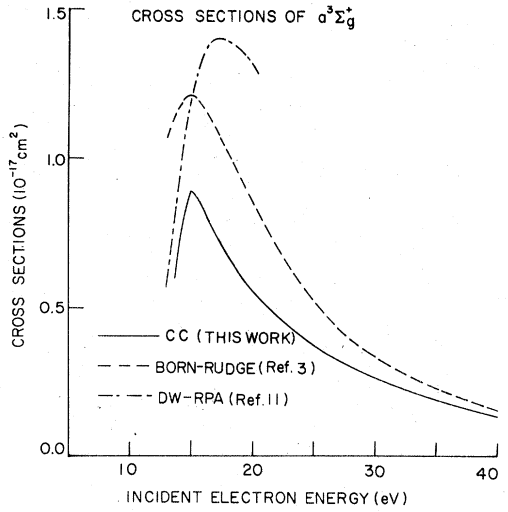

FIG. 5. Excitation cross sections of the $a\,^3\Sigma_g^+$ state calculated by means of (i) close coupling (solid line) of this work; (ii) the Born-Rudge approximation (uniform dashed line) in Ref. 3; (iii) DW-RPA (long-short dashed line) in Ref. 11.

less than a certain critical time, which may be viewed as the range of interaction divided by the velocity of the colliding electron. The $e\,^3\Sigma_u^+$ state has both electrons in bonding orbitals whereas $b\,^3\Sigma_u^+$ involves one antibonding orbital. Thus the $b\,^3\Sigma_u^+$ state has a more diffuse electron-density distribution, hence a larger range of interaction. This may account for the fact that the decline in the $b\,^3\Sigma_u^+$ excitation function sets in at a higher energy. On the other hand, when the Born-Ochkur approximation is used, the $1/k^4$ factor (k being the wave vector) in the scattering-matrix element gives such a steep energy dependence that it obscures the difference in the range of interaction.

2. $a\,^3\Sigma_g^+$ and $c\,^3\Pi_u$

Figure 5 shows the cross sections of $a\,^3\Sigma_g^+$ computed by close coupling, the Born-Rudge approximations,[3] and DW-RPA.[11] The difference in shape of excitation function is not too severe for $a\,^3\Sigma_g^+$ between CC and BR calculations. Again, we see a large difference in magnitude at low energy (~40% at 15 eV) but a better agreement at high energy (~20% at 40 eV). The cross sections by DW-RPA are much larger than CC results (~50%). However, the shift in the position of peak may well be due to the different values of threshold energy used in the calculations.

The cross sections of $c\,^3\Pi_u$ presented in this paper are based on the three-state close-coupling calculations technically, as we included the $X\,^1\Sigma_g^+$ and $c\,^3\Pi_u$ ($\lambda = \pm 1$) states in the scattering equation. However, at one energy (15 eV) we also performed a two-state calculation, from which we obtained a cross section of 5.95×10^{-17} cm^2 as compared with 5.63×10^{-17} cm^2 from the three-state calculation. The slight difference (6%) indicates that the mutual interactions between channels belonging to the $c\,^3\Pi_u$ ($\lambda = +1$) and $c\,^3\Pi_u$ ($\lambda = -1$) states have no great effect on the cross sections. The results of $c\,^3\Pi_u$ cross sections by CC and BR are compared in Fig. 6. Here, the discrepancy is mainly on the magnitude of cross sections. The BR cross sec-

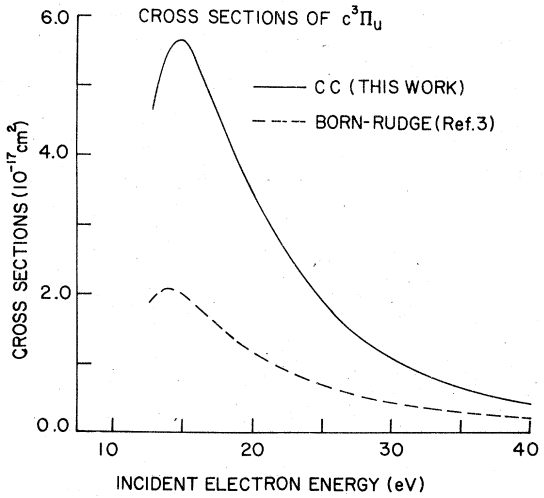

FIG. 6. Excitation cross sections of the $c\,^3\Pi_u$ state calculated by means of (i) the close coupling (solid line) of this work; (ii) the Born-Rudge approximation (dashed line) in Ref. 3.

tions[3] are much smaller than the CC counterpart. Although the discrepancy diminishes with increasing of incident-electron energy, the BR cross section is only one-half of the CC cross section even at 40 eV. We can offer no particular reason for this discrepancy beyond the inadequacy of the Born-type approximation already discussed.

3. *Comparison with experimental dissociation cross sections*

The formation of two H(1s) atoms by electron impact on H_2 arises from direct excitation of $b\,^3\Sigma_u^+$ and from excitation of other triplet states followed by cascade to $b\,^3\Sigma_u^+$. It has been shown in Ref. 3 that $a\,^3\Sigma_g^+$ and $c\,^3\Pi_u$ are the two major cascading states to $b\,^3\Sigma_u^+$ and that $e\,^3\Sigma_u^+$ and $d\,^3\Pi_u$ play only minor roles. Thus we take the sum of the cross sections of $b\,^3\Sigma_u^+$, $a\,^3\Sigma_g^+$, $c\,^3\Pi_u$, and $e\,^3\Sigma_u^+$ as the theoretical cross sections for the dissociation process $H_2 \xrightarrow{e} H(1s)+H(1s)$, which are shown in Fig. 7. Experimentally Corrigan[32] has obtained dissociation cross sections (via the excited states of the neutral H_2 molecule) which cover the formation of the excited-state H(nl) atoms as well as H(1s). In Ref. 3 efforts were made to subtract from Corrigan's data the experimental cross sections for producing the excited-state atoms. The "corrected" experimental data given in Ref. 3 correspond to the formation of two H(1s) atoms and are reproduced in Fig. 7 for comparison with the theoretical values. The agreement is seen to be quite good. However, it must be cautioned that there is a considerable uncertainty in Corrigan's data (see Fig. 2 of Ref. 32) especially at the high-energy side. The close agreement between theory and experiment, therefore, should not be regarded as having much quantitative significance.

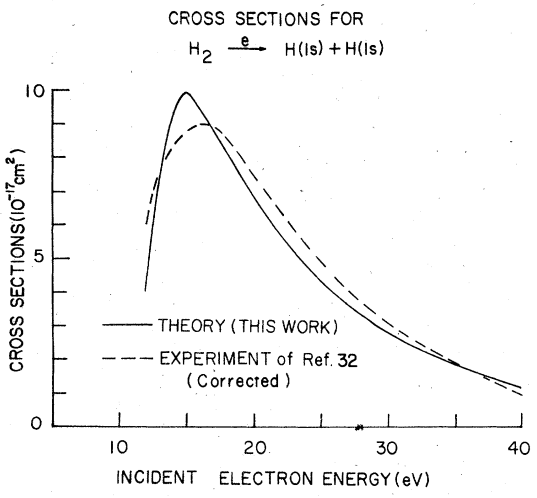

FIG. 7. Theoretical cross sections of this work (solid line) for the dissociation process $H_2 \xrightarrow{e} H(1s)+H(1s)$ as compared with experimental values (dashed line) of Ref. 32 corrected to represent the production of H(1s) atoms only as described in Ref. 3.

4. *Summary*

With a limited number of case studies made here, only a tentative conclusion can be drawn on the performance of the Born-type approximations. Nevertheless, we see a pattern emerging. First, at a moderate energy (say, 20 eV or above) of incident electron the agreement between CC and BR results is reasonable in most cases. While this comparison reaffirms that the Born types are basically "high-energy" approximations, it also puts a limit of their applicability on a more quantitative basis as well. The other is much more serious, that is, at low energy the discrepancy is not only large, neither does it appear to follow any clear trend. We can say neither BR overestimates nor underestimates cross sections since the details of the exchange potential, which must reflect the characteristics of electronic states involved, are lost amid the approximate procedures leading to the Born-Rudge or Born-Ochkur method. Indeed, the present close-coupling calculation shows that the shape of excitation functions is not alike for all triplet states whereas a much higher uniformity was seen from the BR results.

B. Excitation to the $B\,^1\Sigma_u^+$ state

As described in Sec. III A, our close-coupling calculation for the $X\,^1\Sigma_g^+ \rightarrow B\,^1\Sigma_u^+$ excitation has been carried out with the aid of a parallel partial-wave analysis of the Born approximation. The essential assumption made in Sec. III A was that for large l,l',

$$Q^{(CC)}(l,l') \simeq Q^{(Born)}(l,l') \tag{70}$$

with

$$Q(l,l') = \sum_{\Lambda} Q^{\Lambda}(l,l') \ . \tag{71}$$

In order to discuss how this assumption may affect the total excitation cross sections, we display in Tables XI and XII the partial cross sections of Eq. (71) summed over $\Lambda = -6$ to $+6$ at the incident-electron energies of 25 and 100 eV. In addition to the Born and CC cross sections, we also included in these tables a set of cross sections calculated by the close-coupling method without the electron-exchange (CCNE). It is evident from these tables that the partial cross sections $Q(l,l')$ of the singlet state do not decrease with increasing l as rapidly as the triplet counterparts. This is due to the presence of the long-range direct potentials in the singlet-singlet excitation, hence the necessity of a special treatment referred to above. We show

TABLE XI. Partial cross sections[a] $Q(l, l')$ defined as in Eq. (71) for the $B^1\Sigma_u^+$ state at $E = 25$ eV in a_0^2.

	$Q(l, l' = l - 1)$			$Q(l, l' = l + 1)$		
l	CC	CCNE	Born	CC	CCNE	Born
0				0.355(-2)	0.671(-3)	0.887(-2)
1	0.287(-1)	0.943(-1)	0.370(0)	0.329(-1)	0.161(-1)	0.159(-3)
2	0.184(0)	0.468(0)	0.605(0)	0.248(-1)	0.169(-1)	0.320(-2)
3	0.378(0)	0.674(0)	0.533(0)	0.213(-1)	0.162(-1)	0.341(-2)
4	0.351(0)	0.432(0)	0.360(0)	0.639(-2)	0.738(-2)	0.239(-2)
5	0.234(0)	0.238(0)	0.217(0)	0.416(-2)	0.295(-2)	0.124(-2)
6	0.114(0)	0.126(0)	0.122(0)	0.912(-3)	0.107(-2)	0.687(-3)
7	0.685(-1)	0.660(-1)	0.676(-1)		0.384(-3)	0.344(-3)
8		0.347(-1)	0.364(-1)			

[a] Numbers in parentheses indicate powers of 10.

in Tables XI and XII the $Q(l, l' = l - 1)$ and $Q(l, l' = l + 1)$ sequences only, since their contributions to the total cross sections are about 90% and 10%, respectively. For the sequence $l' = l - 1$, the three sets of partial cross sections merge to one another; for example, within 4% at the last entry ($l = 7$). Furthermore, this error will affect only the fraction $(l, l' \geq 7)$ of the total cross section so that the net effect on the total cross section is expected to be much smaller. As to the the $l' = l + 1$ sequence, the convergence is not as good as the $l' = l - 1$ sequence. However, the entire $Q(l, l' = l + 1)$ sequence occupies only 10% of the total, so that any error there will be scaled down by a factor of 10. Therefore we estimate that the total error incurred by our procedure does not exceed 5% or so at 100 eV, and is smaller yet at lower energies of incident electron. The important point to note here is that the difference between the Born and CC calculations manifests mainly in the partial cross sections of small l as shown in Tables XI and XII so that the partial cross sections of large l may be computed by either method without incurring much error. Therefore we replace $Q^{(CC)}(l, l')$ by $Q^{(Born)}(l, l')$ for $(l, l') > 7$ as prescribed by Eq. (29) to obtain the total CC cross sections. The total cross sections by CCNE are obtained in a similar manner.

These total cross sections are shown in Table XIII and in Fig. 8. For comparison we also calculated the cross sections of this state by using the Born-Ochkur approximation (BO). As expected the Born approximation grossly overestimates the cross sections at low energy (by 55% at 25 eV), but at high energy (100 eV) the CC and Born cross sections are within 8% of each other. The poor performance of CCNE should also have been anticipated, since it makes no allowance for the electron exchange. Nevertheless, it is somewhat disappointing to see a substantial difference between CCNE and CC at energies as high as 50 eV. The CCNE and Born approximation give essentially the same cross sections even at 25 eV. It is more difficult to assess the performance of the Born-Ochkur approximation. While it tends to reduce the cross sections below those given by the Born ap-

TABLE XII. Partial cross sections[a] $Q(l, l')$ defined as in Eq. (71) for the $B\ ^1\Sigma_u^+$ state at $E = 100$ eV in a_0^2.

	$Q(l, l' = l - 1)$			$Q(l, l' = l + 1)$		
l	CC	CCNE	Born	CC	CCNE	Born
0				0.948(-3)	0.111(-2)	0.127(-2)
1	0.763(-2)	0.102(-1)	0.113(-1)	0.441(-2)	0.113(-2)	0.987(-4)
2	0.197(-1)	0.146(-1)	0.334(-1)	0.625(-2)	0.192(-2)	0.405(-3)
3	0.223(-1)	0.349(-1)	0.583(-1)	0.574(-2)	0.498(-2)	0.198(-2)
4	0.437(-1)	0.616(-1)	0.791(-1)	0.576(-2)	0.758(-2)	0.368(-2)
5	0.667(-1)	0.863(-1)	0.920(-1)	0.118(-1)	0.870(-2)	0.488(-2)
6	0.887(-1)	0.911(-1)	0.975(-1)	0.795(-2)	0.858(-2)	0.536(-2)
7	0.943(-1)	0.935(-1)	0.967(-1)		0.733(-2)	0.532(-2)
8		0.890(-1)	0.920(-1)			

[a] Numbers in parentheses indicate powers of 10.

TABLE XIII. Total cross sections of the $B\ ^1\Sigma_u^+$ state in units of 10^{-17} cm^2.

Energy (eV)	CC	CCNE	Born	BO
25	4.31	6.31	6.66	5.31
50	4.71	5.41	5.55	5.14
75	4.09	4.30	4.55	4.36
100	3.58	3.69	3.87	3.76

proximation, such a reduction is assured by the formulation.[33] Therefore, at this time we can view the "success" of the Born-Ochkur approximation only as qualitative and phenomenological.

On the other hand, much better agreement between the Born and CC at high energy is encouraging; even at 75 eV the discrepancy is a mere 10%. With this quantitative assessment, the Born approximation now can be utilized to provide cross sections at still higher incident-electron energies.

VI. CONCLUSION

While the basic formalism governing the collision process is identical in electron-atom and electron-molecule cases, the theoretical advancement of molecular collision lags far behind that of the atomic process. There is no denying that this vast gap between the two is directly attributable to the computational difficulties associated with molecules. In this paper we succeeded in devising a computational procedure capable of handling the singlet-singlet and singlet-triplet excitations to the same level of refinement as in the corresponding electron-atom collision theory.

With an application to H_2 molecule, we demonstrated the importance of treating electron exchange properly, by which certain characteristics of each molecular state involved may be brought out. In contrast, only a qualitative feature can be expected from the short-cut methods hitherto applied to electron-molecule collisions such as the Born-type approximation.

Because of the scarcity of excitation measurements for the low excited states of H_2, we were not able to make a close comparison with experiment. However, with this beginning, extension to homonuclear diatomics of the second row is within our reach where greater abundance of experimental data are available. Finally, in understanding collision processes, we believe theory can offer more to electron-molecule processes than atomic cases as the experimental analyses are more complicated and difficult with the former.

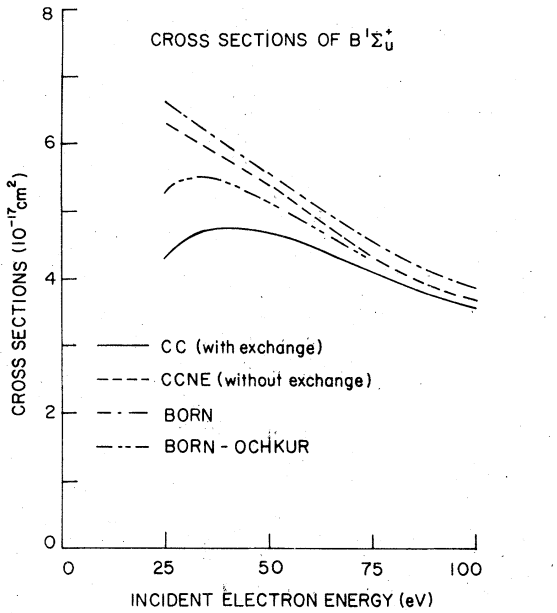

FIG. 8. Excitation cross sections of the $B\ ^1\Sigma_u^+$ state calculated by means of (i) the close coupling *with exchange* (solid line); (ii) the close coupling *without exchange* (uniform dashed line); (iii) the Born approximation (long-short dashed line); (iv) the Born-Ochkur approximation (long-short-short dashed line).

ACKNOWLEDGMENT

The authors wish to express their appreciation to Dr. Edward T. P. Lee for his continued interest in this project and many valuable discussions. This work was supported by DNA (Atmospheric Effects Division) under Subtask No. S99QAX-H1004-W.U.97 LABCEDE Program.

APPENDIX

Throughout this paper we treated the electronic states of a molecule without regard to the vibrational substates associated with each electronic state. It was suggested that cross sections between a pair of electronic-vibrational states may be approximated by means of the Franck-Condon (FC) principle. We now make a brief remark on the effect of the FC approximation on the cross sections. If we had decided not to rely on the FC approximation, the expression for the potentials would have been altered; for example, Eq. (35) would have been replaced by

$$V^e_{\mu v,\mu' v'}(\hat{r}) = \int d\hat{r}\, Y^*_{l,\Lambda-\lambda}(\hat{r}) Y_{l'\Lambda-\lambda'}(\hat{r}) \sum_j f_j \int \chi^*_{\mu v}(R)\chi_{\mu' v'}(R) R^2 dR \int \phi^*_j(\vec{r}', R) \left|\vec{r} - \vec{r}'\right|^{-1} \phi'_j(\vec{r}', R)\, d\vec{r}' \,, \tag{72}$$

where χ_{nv} is the vibrational wave function, and allowance is made for the orbitals to vary with the internuclear separation R. When using the FC approximation, we look for a favorable condition that $\phi(\vec{r},R)$ does not vary much with R. This depends on the characteristic of each electronic state so that we have practically no control over it. Secondly, we look for vibrational overlap $(\chi_{nv}, \chi_{n'v'})$ which is significant only near the vicinity of R_0, the equilibrium separation of the ground state. This is generally satisfactory if the excitation is from the $v=0$ level (usual experimental situation), which, in turn, may compensate for the variation of $\phi(\vec{r},R)$ as well. Another point, which is unrelated to the above, comes from the somewhat arbitrary choice of the threshold (vertical excitation) energy. However, this objectionable point can easily be removed, once the vibrational states of interest are specified.

Regardless of the theoretical formalism adopted in a calculation, we must keep in mind the limitations cited above. In the close-coupling method with the FC approximation, however, we further assume tacitly that the scattering amplitude is proportional to the potentials. It is expected that such a linear relation holds unless the coupling potentials are too strong. We have verified this by performing test calculations, in which potentials are arbitrarily scaled by 0.1, 0.5, and 2.0. The resulting cross sections are within 5% of those expected if the linearity held strictly. Therefore the validity of the FC approximation will remain about the same when used with CC, as with the Born-type calculations.

[1]S. Chung and C. C. Lin, Phys. Rev. A 6, 988 (1972).
[2]S. Chung and C. C. Lin, Phys. Rev. A 9, 1954 (1974).
[3]S. Chung, C. C. Lin, and E. T. P. Lee, Phys. Rev. A 12, 1340 (1975).
[4]D. C. Cartwright and A. Kuppermann, Phys. Rev. 163, 86 (1967).
[5]D. C. Cartwright, Phys. Rev. A 2, 1331 (1970); 5, 1974 (1972).
[6]K. J. Miller and M. Krauss, J. Chem. Phys. 47, 3754 (1967).
[7]S. P. Khare and B. L. Moiseiwitsch, Proc. Phys. Soc. Lond. 88, 605 (1966).
[8]S. P. Khare, Phys. Rev. 157, 107 (1967).
[9]V. I. Ochkur, Zh. Eksp. Teor. Fiz. 45, 734 (1963) [Sov. Phys.-JETP 48, 503 (1964)].
[10]M. R. H. Rudge, Proc. Phys. Soc. Lond. 85, 607 (1965).
[11]T. N. Rescigno, C. W. McCurdy, Jr., V. McKoy, and C. F. Bender, Phys. Rev. A 13, 216 (1976).
[12]J. M. Blatt and L. C. Biedenharn, Rev. Mod. Phys. 24, 258 (1952); I. C. Percival and M. J. Seaton, Proc. Camb. Philos. Soc. 53, 654 (1957); B. H. Bransden and J. S. C. McKee, Proc. Phys. Soc. Lond. A 69, 422 (1956); R. Marriott, Proc. Phys. Soc. Lond. A 72, 121 (1958).
[13]B. L. Moisewitsch and S. J. Smith, Rev. Mod. Phys. 40, 238 (1968); this review article contains an extensive bibliography on close-coupling method.
[14]K. Smith, R. J. W. Henry, and P. G. Burke, Phys. Rev. 147, 21 (1966).
[15]E. R. Smith and R. J. W. Henry, Phys. Rev. A 7, 1585 (1973); and references therein.
[16]L. L. Barnes, N. F. Lane, and C. C. Lin, Phys. Rev. 137, 388 (1965).
[17]D. F. Korff, S. Chung, and C. C. Lin, Phys. Rev. A 7, 545 (1973).
[18]F. E. Fajen, Ph.D. dissertation (The University of Oklahoma, 1968) (unpublished); F. E. Fajen and C. C. Lin, Bull. Am. Phys. Soc. 14, 225 (1969).
[19]K. F. Black and N. F. Lane, in *Abstracts of Papers, Sixth International Conference on the Physics of Electronic and Atomic Collisions, Cambridge, Mass., 1969* (MIT, Cambridge, Mass., 1969), p. 107.
[20]K. F. Black and N. F. Lane, in *Abstracts of Papers, Seventh International Conference on the Physics of Electronic and Atomic Collisions, Amsterdam, The Netherlands, 1971,* edited by L. M. Branscomb *et al.*, (North-Holland, Amsterdam, 1971), p. 332.
[21]U. Fano and D. Dill, Phys. Rev. A 6, 185 (1972).
[22]E. S. Chang and U. Fano, Phys. Rev. A 6, 173 (1972).
[23]For the sake of clarity, we suppress the spin s in the channel index, no confusion arising from this omission.
[24]See, for example, Ref. 14 and K. Smith and L. A. Morgan, Phys. Rev. 165, 110 (1968).
[25]Incident channel index μ is omitted here; however, it is understood that the orthogonality condition applies to scattered waves initiated by all incident channels.
[26]This is a statement that the integrals of Eq. (16) and (17) vanish unless the integrand is an even function with respect to inversion.
[27]For the range of incident-electron energy considered in this paper, it is realistic to use the representation in which Λ is diagonal. See, for example, Ref. 22 for details.
[28]E. U. Condon and G. H. Shortley, *The Theory of Atomic Spectra* (Cambridge University, Cambridge, England, 1963).
[29]S. Huzinaga, J. Chem. Phys. 42, 1293 (1965), Tables V and VI.
[30]C. C. J. Roothaan, Rev. Mod. Phys. 23, 69 (1951); 32, 179 (1960); W. M. Huo, J. Chem. Phys. 45, 1554 (1966).
[31]D. H. Madison and W. N. Shelton, Phys. Rev. A 7, 499 (1973); M. S. Pindzola and H. P. Kelly, *ibid.* 11, 221 (1975).
[32]S. J. B. Corrigan, J. Chem. Phys. 43, 4381 (1965).
[33]See, for example, Eq. (9) of Ref. 1.